Am J Transl Res 2017;9(9):4250-4260
www.ajtr.org /ISSN:1943-8141/AJTR0055299

Original Article

Stachydrine ameliorates pressure overload-induced diastolic heart failure by suppressing myocardial fibrosis

Hui-Hua Chen[1*], Pei Zhao[2*], Wen-Xia Zhao[3], Jing Tian[1], Wei Guo[1], Ming Xu[4], Chen Zhang[1], Rong Lu[1]

[1]Department of Pathology, Shanghai University of Traditional Chinese Medicine, 1200 Cailun Road, Shanghai 201203, China; [2]The Public Experiment Platform, Shanghai University of Traditional Chinese Medicine, 1200 Cailun Road, Shanghai 201203, China; [3]Center of Drug Safety Evaluation Research, Shanghai University of Traditional Chinese Medicine, 1200 Cailun Road, Shanghai 201203, China; [4]Department of Physiology, Shanghai University of Traditional Chinese Medicine, 1200 Cailun Road, Shanghai 201203, China. [*]Equal contributors.

Received April 12, 2017; Accepted August 31, 2017; Epub September 15, 2017; Published September 30, 2017

Abstract: Stachydrine (Sta), a major constituent of *Leonurus japonicus* Houtt, has been reported to possess numerous cardioprotective effects. In this study, we evaluated the effect of Sta on pressure overload-induced diastolic heart failure in rats and investigated the mechanisms underlying the effect. Wistar rats were randomized to transverse aortic constriction (TAC) or sham operation. After 3 days, the rats that underwent TAC were randomized to treatment for a total of four experimental groups (n=10 each group): sham operation, TAC only, TAC + telmisartan (Tel), and TAC + stachydrine (Sta). After 12 weeks, we evaluated left ventricular hypertrophy, function, and fibrosis by echocardiography, pressure-volume loop analysis, and histology. In addition, levels of fibrosis-related proteins in the heart were determined by Western blot analysis. Our results showed that Sta significantly suppressed TAC-induced cardiac hypertrophy, and TAC-induced increases in heart weight/body weight and heart weight/tibial length. In addition, Sta attenuated TAC-induced decreases in left ventricular ejection fraction and improved other hemodynamic parameters. Compared with the TAC only group, rats treated with Sta exhibited significant decreases in interstitial and perivascular fibrosis, TGF-βR1 protein levels, and phosphorylation of Smad2/3; however, protein levels of TGF-β1, TGF-βR2, and Smad4 did not differ significantly between the two groups. Taken together, our results demonstrate that Sta protects against diastolic heart failure by attenuating myocardial hypertrophy and fibrosis via the TGF-β/Smad pathway.

Keywords: Stachydrine, diastolic heart failure, hypertrophy, fibrosis

Introduction

Heart failure is a leading cause of death globally [1]. A substantial proportion of patients with congestive heart failure have a normal or slightly reduced ejection fraction, the prevalence of which is rising [2-5]. Clinical heart failure with normal ejection fraction (HFnEF) or preserved ejection fraction (HFpEF) is referred to as diastolic heart failure (DHF), as defined by the American College of Cardiology and American Heart Association [6]. DHF, which has only recently been identified as a clinical entity, is characterized by impaired myocardial compliance, cardiomyocyte hypertrophy, and myocardial fibrosis, which are directly linked to abnormal diastolic function and myocardial stiffness [7]. There is a growing recognition that heart failure caused by diastolic dysfunction causes significant morbidity and mortality [8]. Although isolated diastolic dysfunction as a cause of heart failure remains controversial, early recognition and appropriate therapy of diastolic dysfunction is advisable to prevent further progression to DHF and death. However, to date no effective therapies or preventive measures for DHF have been developed.

Transforming growth factor-β (TGF-β) has a crucial role in tissue homeostasis and is an important extracellular matrix (ECM) regulator [9]. Disruption of TGF-β signaling has been implicated in many human diseases, including cardiovascular diseases. The isoform TGF-β1 plays an important role in the cardiovascular system, where it is a potent stimulator of collagen-pro-

ducing cardiac fibroblasts and is thought to mediate cardiac fibrosis. The two main TGF-β receptors are TGF-β receptor 1 (TGF-βR1) and TGF-β receptor 2 (TGF-βR2). The binding of TGF-β to TGF-βR2 induces a conformational change in this receptor, which allows dimerization with TGF-βR1 and its phosphorylation. The activated complex induces the phosphorylation of Smad2 and Smad3, which form hetero-oligomeric complexes with Smad4. These complexes then translocate to the nucleus, where they regulate transcriptional responses involved in fibrosis [10-12].

Stachydrine (Sta) is an activated alkaloid that can be isolated from *Leonurus japonicus* Houtt, a traditional Chinese medicine. Results of preclinical studies and clinical trials have demonstrated that the herb exerts cardioprotective effects [13]. For example, aqueous extracts and alkaloids extracted from *L. japonicus* Houtt have beneficial effects on left ventricular (LV) dysfunction and remodeling in rats [14, 15]. Recently, our group showed that Sta attenuates angiotensin II (Ang II)-induced and norepinephrine-induced cardiomyocyte hypertrophy [16, 17]. However, it remains unclear whether Sta can improve pressure overload-induced DHF. Thus, in the present study we evaluated the effects of Sta on pressure overload-induced DHF and investigated the mechanism of action.

Materials and methods

Animals

The study protocol was approved by the Animal Care and Use Committee of Shanghai University of Traditional Chinese Medicine. Male Wistar rats (approximately 150 ± 10 g) were housed in cages with controlled temperature and humidity, 12-h light-dark periods, and free access to water and a standard diet.

Transverse aortic constriction

Transverse aortic constriction (TAC) surgery was used to generate a rat model of pressure overload-induced cardiac hypertrophy and heart failure. Briefly, the rats were placed in a chamber, anesthetized with 5% isoflurane (SurgiVet, MI, USA), and then intubated and ventilated (Harvard, Inspira ASV, Harvard Apparatus, Holliston, MA, USA), delivering tidal volumes of 6 ml. During the procedure, 2.5% isoflurane in 95% oxygen and 5% carbon dioxide was used to maintain anesthesia. The rats were placed supine on a heating pad (World Precision Instruments, Inc., Sarasota, FL, USA), with the temperature maintained at approximately 37°C. The aortic arch was carefully dissected free of the surrounding tissues. To create partial aortic constriction, a stylet made from a bent and blunted 18G intravenous catheter was tied tightly to the aorta between the innominate artery and the left carotid artery using 4-0 silk and then removed. The sternum and the skin incision were closed with 5-0 sutures. The sham operation included all surgical procedures except the ligation. Four weeks later, rats that underwent TAC were evaluated by echocardiography to determine aorta diameter after ligation. Only rats with an aorta diameter <1 mm were used for further study.

Treatments

The rats that underwent TAC were randomized to treatment 3 days after the procedure for a total of four experimental groups (n=10 each group): sham operation, TAC only, TAC + telmisartan (Tel, 5 mg/kg; Boehringer Ingelheim, Shanghai, China), or TAC + Sta (8 mg/kg; National Standard Materials Information Center, Beijing, China). The Tel, Sta, or normal saline (for the sham operation and TAC only groups) was provided once a day by oral gavage for 12 weeks.

Pressure-volume measurements by conductance catheter

Hemodynamic parameters were determined using a 1.9 Fr pressure-volume (PV) conductance catheter (Scisense, Ontario, Canada). Rats were anesthetized with 2.5% isoflurane in 95% oxygen and 5% carbon dioxide. The PV catheter was placed in the left ventricle using an apex approach, as previously described [18-20]. PV data were analyzed using iWorx LabScribe2 data recording and analysis software.

Echocardiographic examination

The rats were anesthetized with 2.5% isoflurane in 95% oxygen and 5% carbon dioxide, and hair on the chest was removed by shaving and depilatory cream. LV function was evaluated by echocardiography using a high-resolution small animal imaging system (Vevo 2100; Vi-

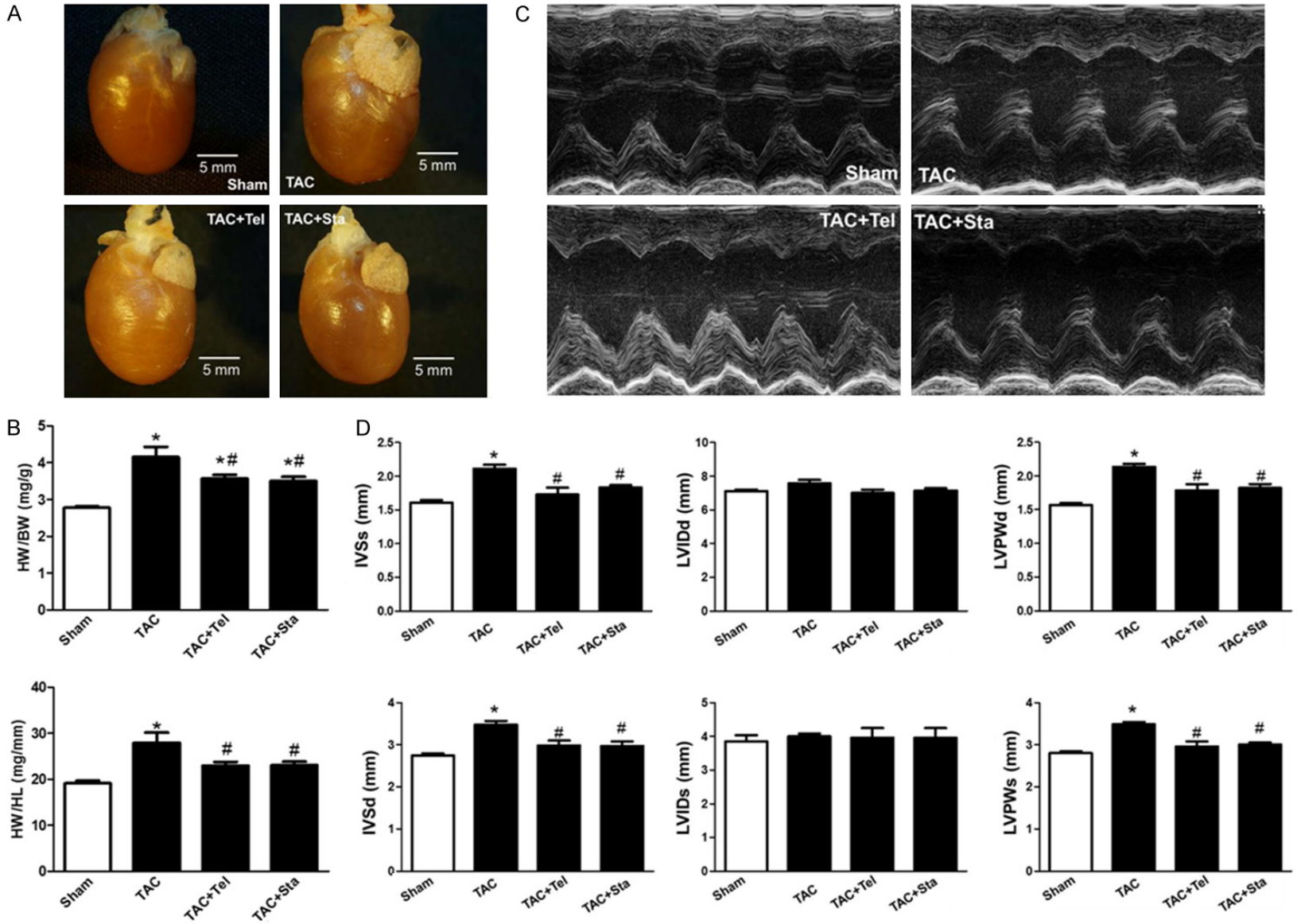

Figure 1. Sta suppressed TAC-induced cardiac hypertrophy. (A) Comparison of heart size (scale bar, 5 mm) in rats that underwent the sham operation, TAC only, or TAC followed by treatment with Tel or Sta. (B) Ratios of heart weight-to-body weight and heart weight-to-tibial length in the four treatment groups. (C) Representative M-mode echocardiographic tracings. (D) Echocardiographic measurements (mean ± SEM). $^{*}P<0.05$ versus sham; $^{\#}P<0.05$ versus TAC only. TAC, transverse aortic constriction; Tel, telmisartan; Sta, stachydrine; HW, heart weight; BW, body weight; TL, tibial length; IVS, interventricular septal; LVID, left ventricular internal dimension; LVPW, left ventricular posterior wall.

sualSonics Inc., Toronto, Canada), with the animal placed in the supine position on a warming platform. Two-dimensional and M-mode echocardiographic studies were performed from short axis view and end-systolic and ventricular dimensions [21].

Western blotting analysis

Heart tissue protein lysates were separated by 10% SDS-PAGE and then transferred to polyvinylidene difluoride membranes (EMD Millipore, Billerica, MA, USA). The membranes were probed overnight at 4°C with primary antibodies against TGF-β1 (Cell Signaling Technology, Danvers, MA, USA), TGF-βR1 (Cell Signaling Technology), TGF-βR2 (Cell Signaling Technology), phosphorylated Smad2/3 (p-Smad2/3; Cell Signaling Technology), Smad2/3 (Cell Signaling Technology), Smad4 (Santa Cruz Biotechnology, Dallas, TX, USA), β-actin (Santa Cruz Biotechnology), and glyceraldehyde 3-phosphate dehydrogenase (GAPDH; Hangzhou MultiSciences, Hangzhou, China). The next day, the membranes were washed and incubated with the appropriate secondary antibody for 1 h at room temperature. After the final wash, signals were detected using the FluorChem E imaging system (ProteinSimple, San Francisco, CA, USA) and a chemiluminescence detection kit (EMD Millipore). Protein band densities were quantified by using an image analysis system and expressed as ratios to GAPDH or β-actin.

Masson's trichrome staining

Heart tissue was fixed in 4% paraformaldehyde overnight at 4°C, rinsed, and transferred to phosphate buffered saline, followed by paraffin embedding. To evaluate fibrosis, sections were stained with Masson's trichrome stain, examined by light microscopy, and photographed at × 400 magnification. Collagen volume fraction (collagen area/total area × 100%) was determined by using Image-Pro Plus 6.0 (Media Cybernetics, Inc., Silver Spring, MD, USA).

Statistical analysis

Data were analyzed using SPSS 18.0, and results are presented as mean ± standard error of the mean (SEM). Data from the experimental groups were compared by one-way analysis of variance followed by Tukey's post hoc analysis, and differences were considered significant at $P<0.05$.

Results

Sta suppressed TAC-induced cardiac hypertrophy

To determine the effect of Sta on TAC-induced cardiac hypertrophy, the heart weight (HW)-to-body weight (BW) ratio and HW-to-tibial length (TL) ratio were calculated, and M-mode echocardiography was used to assess cardiac dimensions. Compared to the sham operation group, rats in the TAC only group exhibited considerable hypertrophy of the whole heart (**Figure 1A**) and higher HW/BW and HW/TL ratios (**Figure 1B**). LV wall thickness (including left ventricular posterior wall [LVPW] and interventricular septal [IVS] thickness) was significantly increased in the systolic and diastolic phases in the TAC only group compared with the sham operation group, whereas the LV internal dimension in the systole and diastole did not differ significantly between the two groups (**Figure 1C**, **1D**). In contrast, the whole heart in Sta-treated rats was considerably smaller, and the HW/BW and HW/TL ratios were decreased compared with the TAC only group. In addition, Sta attenuated TAC-induced LV wall thickening. These results suggest that Sta can prevent pressure overload-induced cardiac hypertrophy.

Sta improved TAC-induced cardiac dysfunction

To assess cardiac function, hemodynamic parameters were determined by PV loop analysis. Characteristic changes in PV relationships were observed at baseline and during inferior vena cava occlusion (**Figure 2A**, **2C**). Compared to the sham operation, TAC significantly attenuated LV ejection fraction (EF), an index of LV systolic function; however, EF remained >50% (**Figure 2B**). TAC also strongly increased potential energy, stroke work, and cardiac output. Compared with the TAC only group, rats that received Sta showed enhanced EF and normalized cardiac output, stroke work, and potential energy. The TAC only group exhibited significantly increased stiffness, isovolumetric relaxation time (Tau Glantz), minimum rate of pressure change (dp/dt_{min}), and end diastolic pressure compared with the sham operation group (**Figure 2D**). However, these changes in diastolic function were attenuated in rats that received Sta after TAC. These results suggest that Sta treatment protects against TAC-induced cardiac dysfunction.

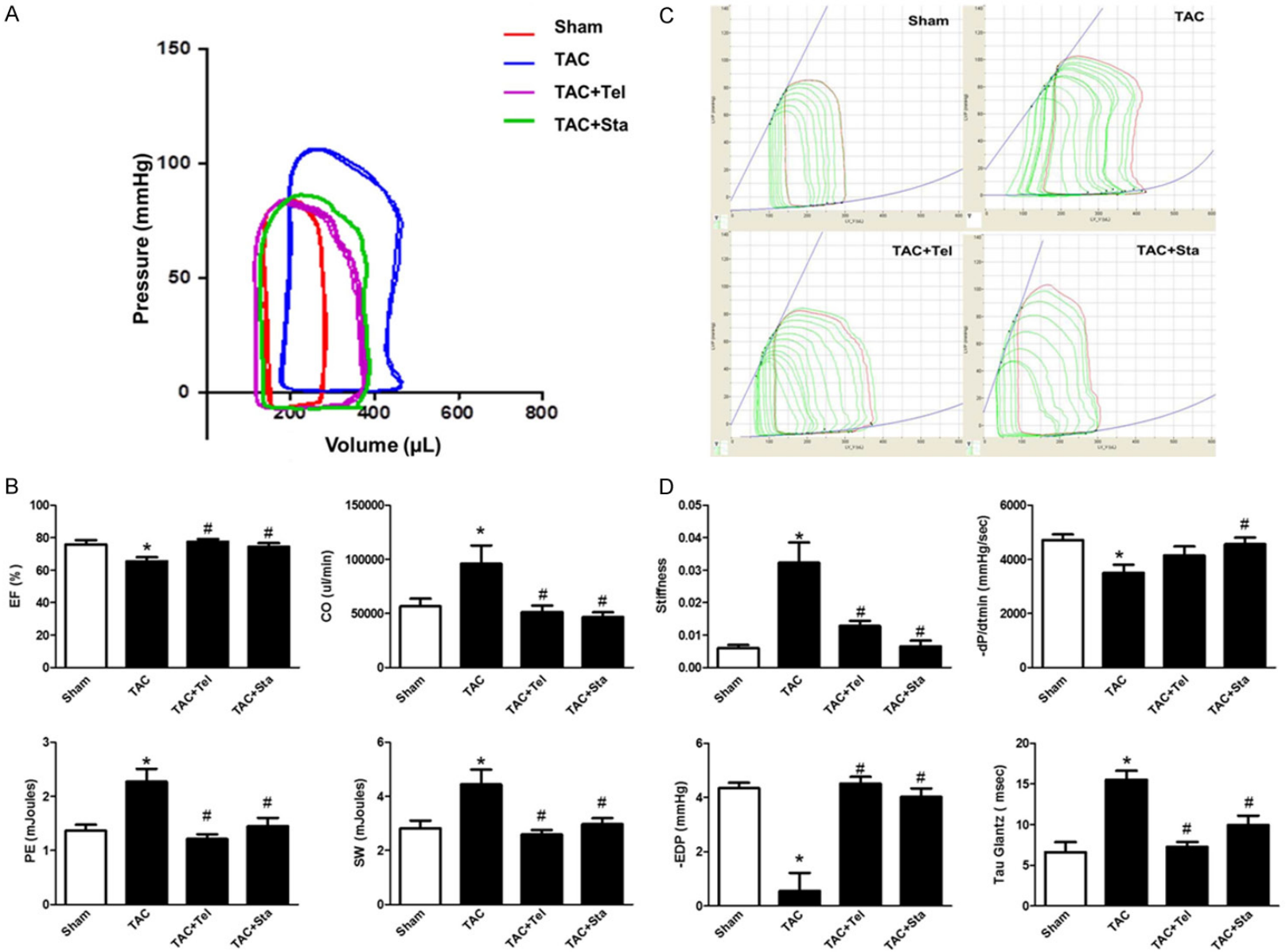

Figure 2. Sta improved TAC-induced diastolic heart failure. (A) Representative pressure-volume loops at baseline. (B) Quantification of hemodynamic parameters at baseline. (C) Representative pressure-volume loops during vena cava occlusion. (D) Quantification of hemodynamic parameters during vena cava occlusion. Results are expressed as mean ± SEM. $^{*}P<0.05$ versus sham; $^{\#}P<0.05$ versus TAC only. TAC, transverse aortic constriction; Tel, telmisartan; Sta, stachydrine. EF, ejection fraction; CO, cardiac output; PE, potential energy; SW, stroke work; EDP, end diastolic pressure; dp/dt_{min}, minimum rate of pressure change.

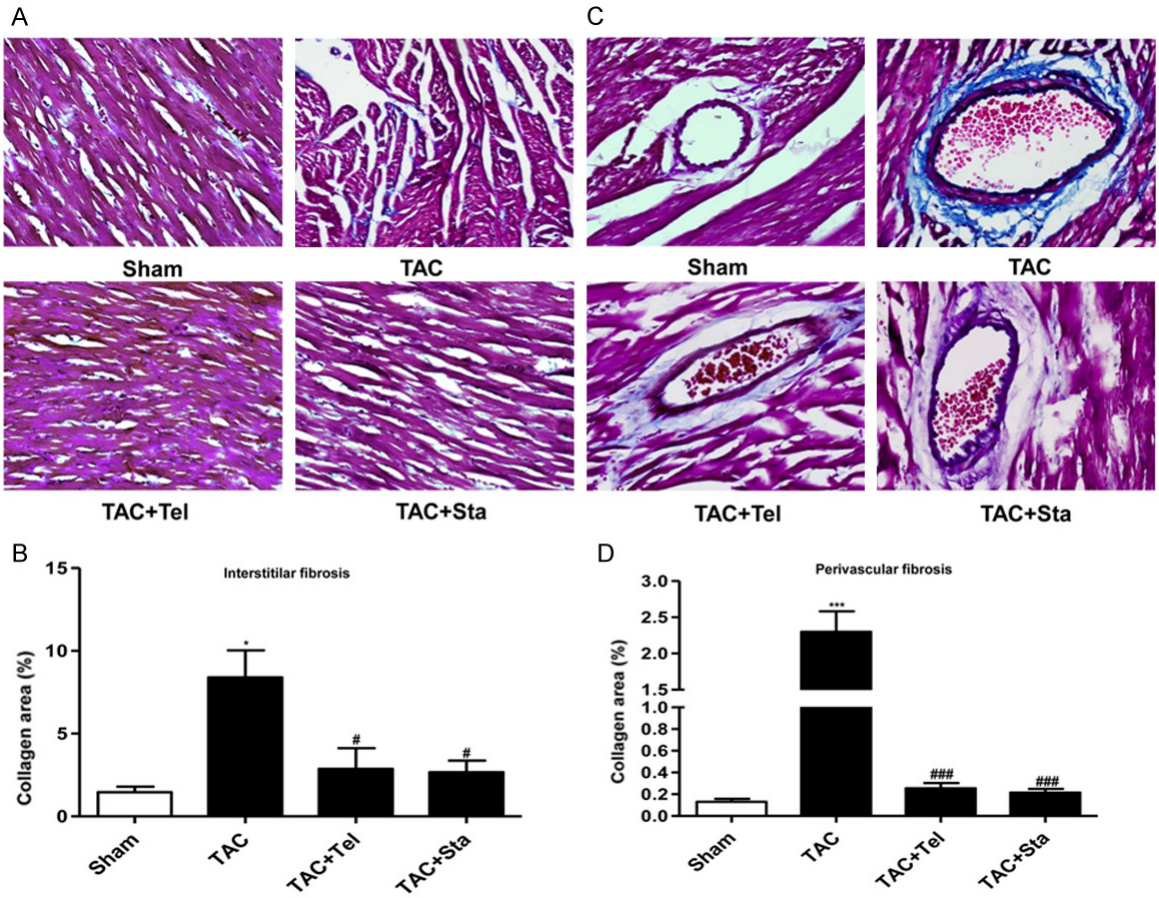

Figure 3. Effect of Sta on TAC-induced myocardial fibrosis. Fibrosis was evaluated by Masson's trichrome staining (n=3), with myocardial cells stained red, and collagenous fibers stained blue. Collagen deposition was quantitatively analyzed as collagen volume fraction (collagen area/total area × 100%). Results are expressed as mean ± SEM. $^{*}P<0.05$, $^{***}P<0.001$ versus sham operation; $^{\#}P<0.05$, $^{\#\#\#}P<0.001$ versus TAC only. TAC, transverse aortic constriction; Tel, telmisartan; Sta, stachydrine.

Sta inhibited TAC-induced myocardial fibrosis

To evaluate fibrosis in the heart, Masson's trichrome staining was used to stain myocardial cells red and collagenous fibers blue (**Figure 3**). Compared with the sham operation group, the TAC only group showed widespread fibrous tissue in interstitial areas (**Figure 3A**, **3B**) and perivascular areas (**Figure 3C**, **3D**). However, rats treated with Sta after TAC showed considerably less fibrous tissue, suggesting that Sta is able to attenuate myocardial fibrosis.

Sta alleviated fibrosis by downregulating TGF-β/Smad signaling

To investigate the mechanism underlying the antifibrotic effects of Sta, protein levels of TGF-β1 and the two main TGF-β receptors (TGF-βR1 and TGF-βR2) in the heart tissue were determined by Western blotting. Our results showed significantly higher TGF-βR1 and TGF-βR2 levels in the TAC only group compared to the sham operation group but no significant difference in TGF-β1 levels. To evaluate Smad signaling, we measured phosphorylation of Smad proteins. Our results showed higher levels of p-Smad2/3 in cardiac tissues of the TAC only group compared to the sham operation group but no significant difference in Smad 4 level between the two groups. In addition, the level of TGF-βR2 appeared to decrease in the Sta-treated rats (**Figure 4**).

Discussion

Previous studies have reported that leonurine, another activated alkaloid found in *Leonurus japonicus* Houtt, significantly improves cardiac function and decreases pulmonary congestion

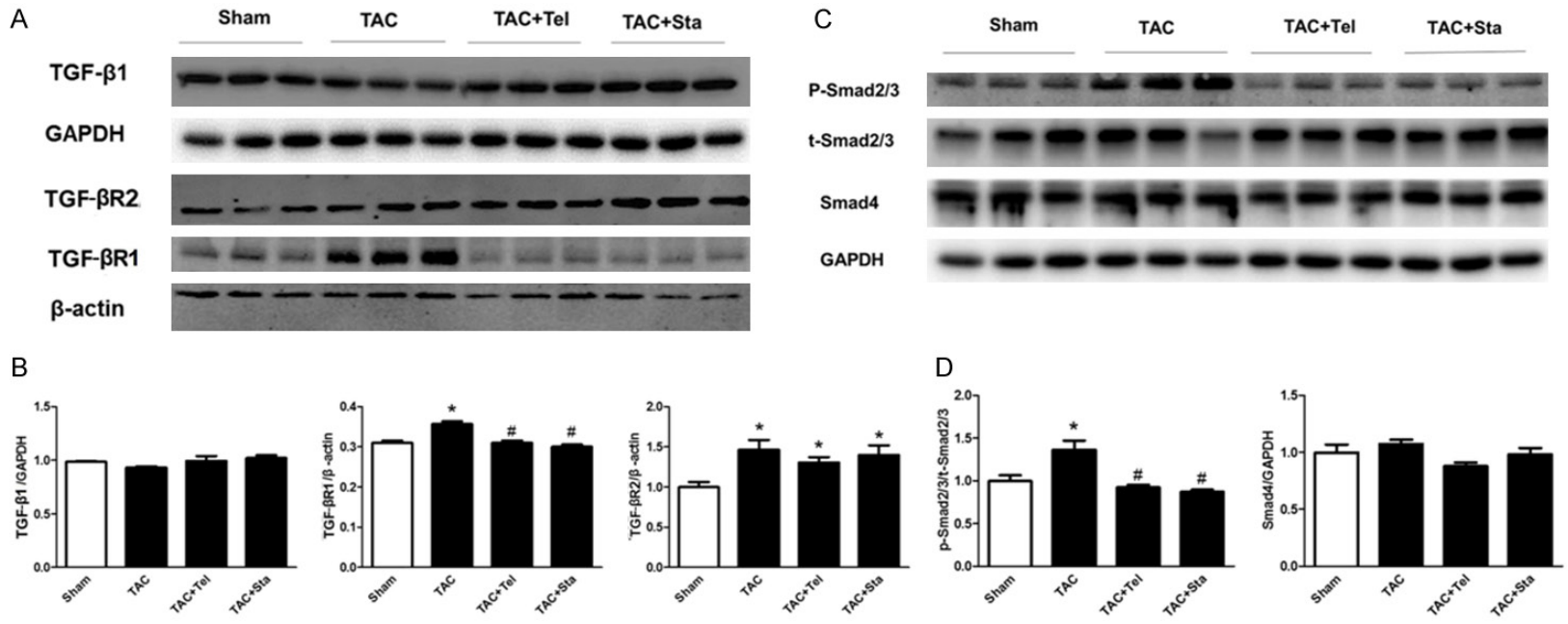

Figure 4. Effect of Sta on fibrosis associated TGF-β/Smad signaling. Protein levels of TGF-β1, TGF-βR1, TGF-βR2, Smad2/3, p-Smad2/3, and Smad4 in heart tissue were determined by Western blotting (n=3). (A and C) Protein bands. (B and D) Quantification of protein levels (mean ± SEM). $^{*}P<0.05$ versus sham; $^{\#}P<0.05$ versus TAC only. TAC, transverse aortic constriction; Tel, telmisartan; Sta, stachydrine; TGF-β1, transforming growth factor-β1; TGF-βR1, transforming growth factor-β receptor 1; TGF-βR2, transforming growth factor-β receptor 2; p-Smad2/3, phosphorylated Smad2/3; t-Smad2/3, total Smad2/3.

in a rat model of chronic myocardial ischemia [22]. Our group provided the first evidence that the L. *japonicus* Houtt alkaloid stachydrine (Sta) inhibits cardiomyocyte hypertrophy in vitro [16, 17]; however, it was not clear whether Sta improves cardiac function in vivo.

In this study we generated a rat model of pressure overload-induced cardiac hypertrophy and heart failure using TAC. This procedure involves tightening a suture around the transverse aorta to increase resistance to blood flow, thereby increasing hemodynamic load on the heart and requiring greater force to maintain normal cardiac output, eventually leading to cardiac hypertrophy [23]. Several studies [24-26] have shown that most patients with DHF exhibit LV hypertrophy. In the present study we detected cardiac hypertrophy 12 weeks after TAC which compensated for the increased hemodynamic load. Results of cardiac catheterization and echocardiography showed diastolic dysfunction in the rats that underwent TAC, as demonstrated by significantly lower cardiac function parameters, such as EF (>50%) and diastolic function. M-mode echocardiography also detected TAC-induced LVPW and IVS hypertrophy in the systolic and diastolic phases. PV loop analysis revealed that the stiffness constant was significantly higher and Tau-Glantz constant was larger in the TAC only group compared with the sham operation group. In addition, the diastolic PV relation was shifted up and to the right in the TAC only group. We found that Sta treatment for 12 weeks after the TAC procedure prevented cardiac hypertrophy and appeared to reverse the myocardial diastolic dysfunction.

In cardiac disease, the heart is subject to changes in composition and structure, often leading to cardiac fibrosis [27]. Fibrosis is also created by the TAC procedure, as demonstrated by assessment of collagen deposition [28, 29]. Although fibrogenesis is initially an effective mechanism of tissue repair, the ongoing remodeling eventually decreases cardiac functionality and leads to heart failure [30]. A major pathological feature of DHF is diastolic dysfunction [8], which is characterized by increased LV stiffness, high LV filling pressure, and myocardial stiffness. Increased LV stiffness has been traced to myocardial fibrosis and increased collagen turnover [31-33]. Myocardial fibrosis, which is associated with reduced microvascular network and disruption of normal myocardial structures, results from excessive deposition of ECM by fibroblasts. The interstitial and perivascular fibrosis ultimately lead to LV hypertrophy, dilatation, and failure [34]. Consistent with the results of previous studies [35, 36], histological analysis of heart tissue 12 weeks after TAC showed interstitial and perivascular fibrosis, which was inhibited by Sta, suggesting that this treatment preserves myocardial compliance and diastolic function.

Our results show that Sta can improve diastolic function, inhibit cardiac hypertrophy, and attenuate fibrosis in rats that underwent TAC, ultimately decreasing LV stiffness and improving LV diastolic filling. To identify the molecular mechanisms responsible for these effects, we evaluated the expression of TGF-β, which has been shown to mediate diastolic dysfunction and cardiac fibrosis when activated [10, 37]. This profibrotic cytokine works synergistically with connective tissue growth factor to promote fibroblast proliferation and the deposition of collagen and fibronectin. In fact, TGF-β is believed to be the most important ECM regulator [9]. In vascular smooth muscle cells, endothelial cells, and fibroblasts, TGF-β1 increases synthesis of ECM proteins, such as fibronectin, collagen, and plasminogen activator inhibitor-1, even at low concentrations [9, 38]. Smad proteins mediate TGF-β signaling [12]. Specifically, TGF-β increases the phosphorylation of Smad2 and Smad3, which then form heterotrimers with Smad4. This complex translocates into the nucleus, binds to Smad-related DNA sequences, and increases the transcription of fibrosis-related genes such as fibronectin, type I collagen, and connective tissue growth factor [11, 12, 39].

In our rat model of DHF we observed increased activation of TGF-βR1 and TGF-βR2 and phosphorylation of Smad2 and Smad3 in heart tissue. These results are consistent with previous studies describing pressure overload-induced cardiac fibrosis via TGF-β1 signaling [40]. In addition, protein levels of Smad4 appeared to increase in the DHF rats; however, this increase was not significant. Our results suggest that Sta improves cardiac fibrosis by decreasing levels of TGF-βR1, TGF-βR2, and p-Smad2/3. Because Ang II-mediated upregulation of TGF-β induces myocardial fibrosis [39], we used telmisartan (Tel), which inhibits angiotensin II type 1 receptor, as a positive control. Our

results showed that Tel inhibited the TAC-induced increase in TGF-βR1 and p-Smad2/3, which supports the involvement of TGF-β/Smad pathways in pressure overload-induced myocardial fibrosis.

Myocardial fibrosis can increase myocardial compliance and myocardial stiffness [41], but our results indicate that treatment with Sta can decrease TGF-β/Smad activation and interstitial and perivascular fibrosis, ultimately decreasing myocardial stiffness and myocardial compliance. This appears to be the main mechanism by which Sta improves diastolic function. Further studies are needed to better understand the antifibrotic and cardioprotective effects of Sta.

Conclusions

Our findings suggest that stachydrine, an alkaloid found in *L. japonicus* Houtt, protects against TAC-induced myocardial hypertrophy and cardiac dysfunction by inhibiting cardiac fibrosis. These findings may provide evidence to support the clinical application of *L. japonicus* Houtt in DHF.

Acknowledgements

This study was funded by the National Natural Science Foundation of China (NO: 30973821; 81373858).

Disclosure of conflict of interest

None.

Address correspondence to: Chen Zhang and Rong Lu, Department of Pathology, Shanghai University of Traditional Chinese Medicine, 1200 Cailun Road, Shanghai 201203, China. Tel: +86-021-51322133; Fax: +86-021-51322133; E-mail: zhangchen@shutcm.edu.cn (CZ); lurong@shutcm.edu.cn (RL)

References

[1] Benjamin EJ, Blaha MJ, Chiuve SE, Cushman M, Das SR, Deo R, de Ferranti SD, Floyd J, Fornage M, Gillespie C, Isasi CR, Jiménez MC, Jordan LC, Judd SE, Lackland D, Lichtman JH, Lisabeth L, Liu S, Longenecker CT, Mackey RH, Matsushita K, Mozaffarian D, Mussolino ME, Nasir K, Neumar RW, Palaniappan L, Pandey DK, Thiagarajan RR, Reeves MJ, Ritchey M, Rodriguez CJ, Roth GA, Rosamond WD, Sasson C, Towfighi A, Tsao CW, Turner MB, Virani SS, Voeks JH, Willey JZ, Wilkins JT, Wu JHY, Alger HM, Wong SS, Muntner P. Heart disease and stroke statistics-2017 update: a report from the American heart association. Circulation 2017; 135: e146-e603.

[2] Steinberg BA, Zhao X, Heidenreich PA, Peterson ED, Bhatt DL, Cannon CP, Hernandez AF, Fonarow GC. Trends in patients hospitalized with heart failure and preserved left ventricular ejection fraction: prevalence, therapies, and outcomes. Circulation 2012; 126: 65-75.

[3] Owan TE, Hodge DO, Herges RM, Jacobsen SJ, Roger VL, Redfield MM. Trends in prevalence and outcome of heart failure with preserved ejection fraction. N Engl J Med 2006; 355: 251-259.

[4] Alsamara M, Alharethi R. Heart failure with preserved ejection fraction. Expert Rev Cardiovasc Ther 2014; 12: 743-750.

[5] Polsinelli VB, Shah SJ. Advances in the pharmacotherapy of chronic heart failure with preserved ejection fraction: an ideal opportunity for precision medicine. Expert Opin Pharmacother 2017; 18: 399-409.

[6] Yancy CW, Jessup M, Bozkurt B, Butler J, Casey DE, Drazner MH, Fonarow GC, Geraci SA, Horwich T, Januzzi JL, Johnson MR, Kasper EK, Levy WC, Masoudi FA, McBride PE, McMurray JJV, Mitchell JE, Peterson PN, Riegel B, Sam F, Stevenson LW, Tang WHW, Tsai EJ, Wilkoff BL. 2013 ACCF/AHA guideline for the management of heart failure: a report of the American College of Cardiology Foundation/American Heart Association Task Force on practice guideline. Circulation 2013; 128: e240.

[7] Querejeta R, López B, González A, Sánchez E, Larman M, Martínez Ubago JL, Díez J. Increased collagen type I synthesis in patients with heart failure of hypertensive origin: relation to myocardial fibrosis. Circulation 2004; 110: 1263.

[8] Nicoara A, Jones-Haywood M. Diastolic heart failure: diagnosis and therapy. Curr Opin Anaesthesiol 2016; 29: 61-67.

[9] Leask A, Abraham DJ. TGF-β signaling and the fibrotic response. FASEB J 2004; 18: 816-827.

[10] Ruiz-Ortega M, Rodriguez-Vita J, Sanchez-Lopez E, Carvajal G, Egido J. TGF-beta signaling in vascular fibrosis. Cardiovasc Res 2007; 74: 196-206.

[11] Rodríguez-Vita J, Sánchez-López E, Esteban V, Rupérez M, Egido J, Ruiz-Ortega M. Angiotensin II activates the Smad pathway in vascular smooth muscle cells by a transforming growth factor-β–independent mechanism. Circulation 2005; 111: 2509.

[12] Hirofumi Ikedo, Kiyoshi Tamaki, Seiji Ueda, Seiya Kato, Makiko Fujii, Peter Ten Dijke, Seiya Okuda. Smad protein and TGF-β signaling in

vascular smooth muscle cells. Int J Mol Med 2003; 11: 645-650.
[13] Liu Xin-Hua, Xin Hong, Zhu Yi-Zhun. More than a "mother-benefiting" herb: cardioprotective effect of Herba leonuri. Sheng Li Xue Bao 2007; 59: 578-584.
[14] Jiang SY, Huang PX, Wei HC, Zhang C, Wang JH, Wu LQ. Effects of alkaloid of Leonurus Heteropyllus Sweet on heart function after myocardial infarction in rats. Shanghai J Tradit Chin Med 2006; 40: 53-56.
[15] Zhang C, Liu Y, Lu R, Guo W, Wei HC. Effects of aqueous extract of Leonurus heterophyllus on expression of myocardial collagen in rats of ventricular remodeling. Acta Universitatis Traditionis Medicalis Sinensis Pharmacologiaeque Shanghai 2011; 25: 76-79.
[16] Zhang C, Shan XL, Liao YL, Zhao P, Guo W, Wei HC, Lu R. Effects of stachydrine on norepinephrine-induced neonatal rat cardiac myocytes hypertrophy and intracellular calcium transients. BMC Complement Altern Med 2014; 14: 474.
[17] Guo, W, Zhang C, Liu Y, Lu R, Wei HC. Effect of Leonurus stachydrine on myocardial cell hypertrophy. Zhong Yao Cai 2012; 35: 940-943.
[18] Faber MJ, Dalinghaus M, Lankhuizen IM, Steendijk P, Hop WC, Schoemaker RG, Duncker DJ, Lamers JMJ, Helbing WA. Right and left ventricular function after chronic pulmonary artery banding in rats assessed with biventricular pressure-volume loops. Am J Physiol Heart Circ Physiol 2006, 291: H1580-1586.
[19] Pacher P, Nagayama T, Mukhopadhyay P, Bátkai S, Kass DA. Measurement of cardiac function using pressure-volume conductance catheter technique in mice and rats. Nat Protoc 2008; 3: 1422-1434.
[20] Wahlquist C, Jeong D, Rojas-Muñoz A, Kho C, Lee A, Mitsuyama S, van Mil A, Jin Park W, Sluijter JPG, Doevendans PAF, Hajjar RJ, Mercola M. Inhibition of miR-25 improves cardiac contractility in the failing heart. Nature 2014; 508: 531-535.
[21] Condorelli G, Morisco C, Stassi G, Notte A, Farina F, Sgaramella G, de Rienzo A, Roncarati R, Trimarco B, Lembo G. Increased cardiomyocyte apoptosis and changes in proapoptotic and antiapoptotic genes bax and bcl-2 during Left ventricular adaptations to chronic pressure overload in the rat. Circulation 1999; 99: 30713078.
[22] Liu X, Pan L, Gong Q, Zhu Y. Leonurine (SCM-198) improves cardiac recovery in rat during chronic infarction. Eur J Pharmacol 2010; 649: 236-241.
[23] Arany Z, Novikov M, Chin S, Ma Y, Rosenzweig A, Spiegelman BM. Transverse aortic constriction leads to accelerated heart failure in mice lacking PPAR-γ coactivator 1α. Proc Natl Acad Sci U S A 2006; 103: 10086-10091.
[24] Aurigemma GP, Gaasch WH. Clinical practice. Diastolic Heart Failure. N Engl J Med 2004; 351: 1097-1105.
[25] Reed AL, Tanaka A, Sorescu D, Liu H, Jeong EM, Sturdy M, Walp ER, Dudley SC Jr, Sutliff RL. Diastolic dysfunction is associated with cardiac fibrosis in the senescence-accelerated mouse. Am J Physiol Heart Circ Physiol 2011; 301: H824-H831.
[26] Gaasch WH. Deliberations on diastolic heart failure. Am J Cardiol 2017; 119: 138-144.
[27] van Spreeuwel ACC, Bax NAM, van Nierop BJ, Aartsma-Rus A, Goumans MTH, Bouten CVC. Mimicking Cardiac Fibrosis in a Dish: Fibroblast density rather than collagen density weakens cardiomyocyte function. J Cardiovasc Transl Res 2017; 10: 116-127.
[28] Verhaart IE, van Duijn RJ, den Adel B, Roest AA, Verschuuren JJ, Aartsma-Rus A, van der Weerd L. Assessment of cardiac function in three mouse dystrophinopathies by magnetic resonance imaging. Neuromuscul Disord 2012; 22: 418-426.
[29] Stuckey DJ, McSweeney SJ, Thin MZ, Habib J, Price AN, Fiedler LR, Gsell W, Prasad SK, Schneider MD. T_1 mapping detects pharmacological retardation of diffuse cardiac fibrosis in mouse pressure-overload hypertrophy. Cir Cardiovasc Imaging 2014; 7: 240-249.
[30] Porras AM, Hutson HN, Berger AJ, Masters KS. Engineering approaches to study fibrosis in 3-D in vitro systems. Curr Opin Biotechnol 2016; 40: 24-30.
[31] Abbate A, Arena R, Abouzaki N, Van Tassell BW, Canada J, Shah K, Biondi-Zoccai G, Voelkel NF. Heart failure with preserved ejection fraction: refocusing on diastole. Int J Cardiol 2015; 179: 430-440.
[32] Periasamy M, Janssen PM. Molecular basis of diastolic dysfunction. Heart Fail Clin 2008; 4: 13-21.
[33] van Heerebeek L, Franssen CP, Hamdani N, Verheugt FW, Somsen GA, Paulus WJ. Molecular and cellular basis for diastolic dysfunction. Curr Heart Fail Rep 2012; 9: 293-302.
[34] Bauersachs J. Regulation of myocardial fibrosis by MicroRNAs. J Cardiovasc Pharmacol 2010; 56: 454-459.
[35] Xia Y, Lee K, Li N, Corbett D, Mendoza L, Frangogiannis NG. Characterization of the inflammatory and fibrotic response in a mouse model of cardiac pressure overload. Histochem Cell Biol 2009; 131: 471-481.
[36] Li XM, Ma YT, Yang YN, Liu F, Chen BD, Han W, Zhang JF, Gao XM. Downregulation of survival signalling pathways and increased apoptosis in the transition of pressure overload-induced

cardiac hypertrophy to heart failure. Clin Exp Pharmacol Physiol 2009; 36: 1054-1061.
[37] Aziz F, Tk LA, Enweluzo C, Dutta S, Zaeem M. Diastolic heart failure: a concise review. J Clin Med Res 2013; 5: 327-334.
[38] Li CJ, Lv L, Li H, Yu DM. Cardiac fibrosis and dysfunction in experimental diabetic cardiomyopathy are ameliorated by alpha-lipoic acid. Cardiovasc Diabetol 2012; 11: 73-73.
[39] Wang W, Huang XR, Canlas E, Oka K, Truong LD, Deng C, Bhowmick NA, Ju W, Bottinger EP, Lan HY. Essential role of Smad3 in angiotensin II–induced vascular fibrosis. Circ Res 2006; 98: 1032-1039.
[40] Zhao L, Mi Y, Guan H, Xu Y, Mei Y. Velvet antler peptide prevents pressure overload-induced cardiac fibrosis via transforming growth factor (TGF)-β1 pathway inhibition. Eur J Pharmacol 2016; 783: 33-46.
[41] Rastogi S, Mishra S, Zacà V, Alesh I, Gupta RC, Goldstein S, Sabbah HN. Effect of long-term monotherapy with the aldosterone receptor blocker eplerenone on cytoskeletal proteins and matrix metalloproteinases in dogs with heart failure. Cardiovasc Drugs Ther 2007; 21: 415-422.